



The Structure of the Onega Downthrown Block and Adjacent Geological Objects According to the Microseismic Sounding Method

KONSTANTIN B. DANILOV¹

Abstract—The geological structure of the major part of the Arkhangelsk region in the North–West Russia has been poorly studied. In the present work, the microseismic sounding method was, for the first time, used to carry out a detailed geological–geophysical survey in the region. The particles motion study confirmed the results of mathematical modeling of the smallest imaged heterogeneity and resolution of the method. The microseism stability study allowed to determine the amount of error of the microseismic sounding method which is 1–2 dB. Two geophysical cross sections of the north-eastern and south-western boundaries of the Onega downthrown block were studied. The method was shown to allow obtaining seismic images with a high precision in the horizontal direction at relatively low costs in terms of time and finances. The obtained data provided additional information about the structure of the crust, which was consistent with the known geological and geophysical information for the surveyed area. Based on the data, it was concluded that the main reasons of the dissonance of geological information were most likely the division of the downthrown block into the northern and southern blocks and horizontal displacement of the layer to the North at a depth ranging from 3 to 5 km. It was suggested that the most active tectonic processes, including eruptions of ancient volcanoes, occurred in the northern block. Two benches at the studied downthrown block were allocated at the depths of 5 and 10 km.

Key words: Microseism, sounding, amplification, particles motion, errors.

1. Introduction

The Earth's crust within the Arkhangelsk region of Russia has been studied rather unevenly. The most studied areas are those where the diamond

fields and oil reservoirs are found, and the number of research works devoted to these areas in the Arkhangelsk region is large. To study the geological environment, it is desired to use methods allowing to obtain the geophysical information at relatively low costs in terms of time and finances. In recent years, the methods relying on microseismic vibrations have been actively developed and exploited. A detailed review and comparison of the methods can be found in various research works (Bonnetfoy-Claudet et al. 2006; Gorbatikov et al. 2008b; Rawlinson et al. 2010). Among the methods, the microseismic sounding method (MSM) is of particular interest due to the high precision of determining vertical borders. The reason of the high precision is the site amplification analyzing. Earlier a number of researchers have used the site amplification of Rayleigh waves from earthquakes for geological environment studies (Dalton and Ekström 2006; Lin et al. 2012; Dalton et al. 2014; Eddy and Ekström 2014). A wide range of Rayleigh waves presents permanently in microseisms, that determine the differences of site amplification of Rayleigh waves from earthquakes and the site amplification of microseism (Gorbatikov and Tsukanov 2011). But the fundamental physical principle underlying the local amplification is the same. In order to estimate the theory correctness and the practicality of MSM, the particle motion and the stability of microseism were analyzed. In the present work, MSM was evaluated for investigation of the Earth's crust in the area of the Onega downthrown block in the northern Arkhangelsk region near the Onega Peninsula. The profiles for Palovo–Samoded and Samoded–Malinovka are shown in Fig. 1.

¹ Federal Center for Integrated Arctic Research, Severnoy Dviny Emb., 23, 163000 Arkhangelsk, Russia. E-mail: danilov.kostea@gmail.com

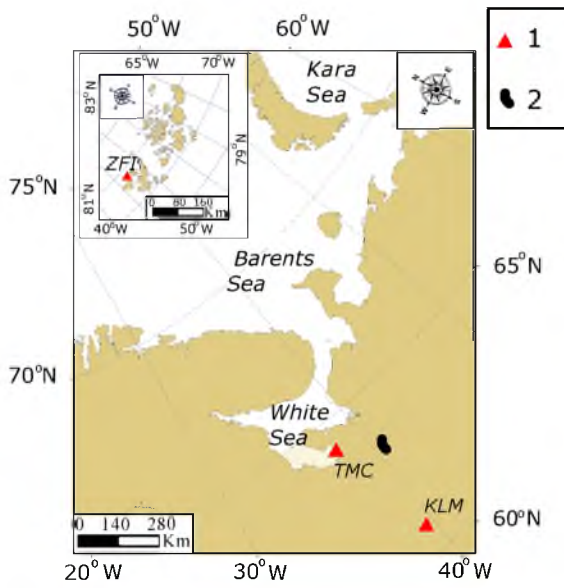


Figure 1

Region of work. 1 seismic station analyzed for stability assessment of microseism, 2 profiles

2. An Overview of the Microseismic Sounding Method

Microseisms are the result of interference of seismic waves of various types, moving as a separate wave train of limited duration. On the one hand, regularities of moving wave trains are well studied. On the other hand, proportions of each type of waves, amplitudes, initial phases, and duration of these wave trains are unknown. As a result, there are two approaches to the analysis of microseisms. The first one is based on the deterministic properties of seismic waves, whereas the second one is based on statistical properties (Gorbatikov and Tsukanov 2011). The methods pertaining to the first group are usually aimed at the experimental determination of the dispersion characteristics (Asten and Henstridge 1984; Horike 1985). The drawbacks of the methods are the difficulties to identify the velocity heterogeneity without sufficient wave travel and labor intensity. The methods pertaining to the second group are based on the correlative correspondence between stable parameters of microseisms and geologic features. Those transient-free parameters may be frequencies and amplitudes at spectral peaks (Kanai and Tanaka 1954; Asten 1978; Katz and Bellon

1978). It should be noted that these methods are somewhat less objective due to the need of making a number of assumptions about the properties of microseisms.

The microseismic sounding method (MSM) used in the present work belongs to the second group of methods. The method was developed by Gorbatikov et al. (2008b) and Gorbatikov and Tsukanov (2011) based on the results of the experiments carried out in the period between 2000 and 2007. The purpose of those experiments was to study space distribution of spectral amplitude of microseisms. As the outcome of experiments, the influence of geological heterogeneities on the intensity variation of microseisms at certain frequencies was revealed. These intensity variations were registered at distances smaller than a wavelength. The important fact is that a similar effect was observed for both the near-surface geological heterogeneity and the heterogeneity at a depth of ten kilometers.

Further, the observed regularities were studied using test geological objects and mathematical models. Surface wave was found to be the dominant microseism mode at a certain distance from the signal source (Nogoshi and Igarashi 1971; Bath 1974; Monakhov 1977). As a consequence, microseisms were conceptualized as a Rayleigh wave field. However, the composition of the natural microseisms is a challenging issue. Vinnik (1968) found that the natural microseismic field may contain up to 60% of body waves. In an ideal case, the dominant mode must be controlled in every point of measurement. However, the body wave amplification is dependent on many factors. Consequently, the effect of the body wave on the MSM method should be studied separately. In the work, system of saline domes, faults, and gradual sinking of the foundation were investigated. According to the results of the investigations, two regularities were identified (Gorbatikov et al. 2008a, b):

1. power spectrum amplitudes of waves of Rayleigh increases when passing through low-velocity heterogeneities and decreases when passing through high-velocity heterogeneities;
2. the greatest change in intensity is observed for wavelengths twice the size of the cover thickness of the heterogeneity. This can be explained by the

fact that a shear stress zone of Rayleigh wave is located at the depth roughly equivalent to half of the length of a wave. As this takes place, the shift zone is located closer to the surface.

In the microseismic sounding method it is necessary to define indicative spectrum of microseisms. To be able to apply the method correctly, the sources of microseisms and their intensity were stable during signal accumulation. In a work by Gorbatikov and Stepanova (2008), it was shown that the period of stationarity of microseisms for the frequency range of 0.12–1.1 Hz was normally equal to 1.5 h.

More recently, a detailed mathematical modeling of Rayleigh wave propagation in a heterogeneous environment was carried out (Gorbatikov and Tsukanov 2011). Based on the results of the modeling, the following facts were identified: the rate of minimal marked heterogeneity was equal to 3–4% of the wavelength; horizontal resolution was equal to a quarter of the wavelength; vertical resolution was equal to a third of the wavelength. The study of the heterogeneity was carried out for the velocities contrast of 10%. It should be noted that the variation of velocities contrast may affect the rate of minimal marked heterogeneity. It was shown that vertical borders of the objects comparable with the length of a wave could be identified with high precision. In addition, the dependence of the coefficient of the depth adjustment on the contrast in velocity was investigated. The obtained values essentially lie in the range of 0.4–0.7. For the zero velocity contrast, the depth adjustment coefficient for the top of the structure was equal to ca. 0.51, and for the center of the inclusion it was equal to ca. 0.43. These values agree well with the previous experimental results (Gorbatikov et al. 2008a, b). Thus, using average dispersive dependences for the object of interest it is fair to use a coefficient of the depth adjustment of 0.4. In the case of existence of contrast objects, it is possible to correct the coefficient. The dispersive dependence characteristics of the studied region can be obtained, for example, from the data from deep seismic sounding (DSS), the method of the receiving functions for the Ps waves, cross-correlation methods, etc.

The experimental results (Gorbatikov et al. 2008a, 2013; Danilov 2011; Francuzova et al.

2013) showed that in some cases the resolution of the method increases. According to the results obtained from the mathematical models (Gorbatikov et al. 2013), the resolution of the method increases considerably if the Poisson coefficient in the inclusion and the S-wave velocity contrast are approaching zero. In turn, the proximity of Poisson coefficient to zero means that the medium in the inclusions must be fractured (Gorbatikov et al. 2013). The effect of “super resolution” made it possible to reveal two large intrusive bodies beneath the El Hierro Island (Gorbatikov et al. 2013). Similar to the results obtained for the El Hierro Island, the vertical high-intensity zone was also found in the Onega Peninsula Arkhangelsk region of Russia using MSM (Francuzova et al. 2013). These low-velocity zones can also be ancient volcanoes.

The main advantage of the method is its high precision of determining vertical borders. The high lateral resolution is a result of the use of amplitude information. The waves of different types are developed as a result of Rayleigh wave scattering on inhomogeneity. However, these different types of waves cannot be distinguished near the heterogeneity. In this case, the amplitude is the source of heterogeneity information available for the analysis.

It should be noted that similar statements have been made by independent researches more recently. Taylor et al. (2009) have shown that the shape and amplitude of individual station resonance peaks appeared to be correlated with local geology. The research conducted by Lin et al. (2012) and Eddy and Ekström (2014) amplification of earthquake Rayleigh waves has the following features:

- amplification of waves primarily due to changes in the velocity properties of the environment;
- amplification of Rayleigh waves increases when passing through low-velocity heterogeneities and decreases when passing through high-velocity heterogeneities;
- amplification due to local geology can be used to refine current elastic models of the crust and upper mantle;
- surface wave amplification is more sensitive than phase velocity.

The above-mentioned recent findings reported by Taylor et al. (2009), Lin et al. (2012), and Eddy and Ekström (2014) support earlier studies conducted by Gorbatikov et al. (2008a, b, 2009, 2011, 2013) and Gorbatikov and Tsukanov (2011). The key advantage of research by Lin et al. (2012) and Eddy and Ekström (2014) is that the Rayleigh wave was analyzed directly. The distinctive feature of researches of the Gorbatikov et al. (2008a, b, 2009, 2011, 2013) is that in the surveyed environment there was no velocity properties smoothing. Good agreement between the results of independent earthquakes (Lin et al. 2012; Eddy and Ekström (2014) and microseisms (Gorbatikov et al. 2008a, b, 2011, 2013) studies confirmed their authenticity. The advantage of microseism analysis is that the Rayleigh wave amplification is observed directly above the heterogeneity (Gorbatikov and Tsukanov 2011). It is also important to note that the microseismic sounding method avoids the necessity to consider the effects of focusing/defocusing and attenuation.

Since the method is sensitive to the temporal variations of microseism, a reference station should be used to eliminate the effects of the temporal variations (Gorbatikov et al. 2008a, b). Additionally, the station records can be used as a “reference” for rejecting noise.

Procedure of the data processing consists of the power spectra computation for each mobile and the reference measurement points, and calculate the relative intensity (I_{fi}) for each point and each frequency. The relative intensity is the ratio of mobile station spectral amplitude to the reference station spectral amplitude expressed in decibel (Gorbatikov et al. 2008a, b, 2013; Gorbatikov and Tsukanov 2011):

$$I_{fi} = 20 \lg \frac{A_{fi}^m}{A_{fi}^r}, \quad (1)$$

where A_{fi}^m, A_{fi}^r , spectral amplitudes for seismograms recorded at the i th measurement point of the mobile (m) and reference (r) stations at the considered frequency (f). The next step (Gorbatikov et al. 2013) is the determination of the depth (h) to be sounded as:

$$h(f) = KVr(f)/f,$$

where $h(f)$, depth of microseismic sounding for a frequency f ; $Vr(f)$, Rayleigh wave velocity for a frequency f ; K , numerical coefficient equal to 0.4.

The result of the data processing by the microseismic sounding method is the geophysical imaging shown in the distribution of relative intensity of microseisms along the profile and by depth (I_{hi}). Zones with a higher relative microseism intensity represent an area with relatively reduced velocity properties, and vice versa.

General principles of MSM correspond to a matter of common knowledge. MSM allows to develop a seismic image of the environment based on the analysis of seismograms, which is consistent with the known fact that the character of seismograms is defined by the geophysical features of registration point. In the MSM, it is assumed that the low-velocity heterogeneities cause an increase in the microseism intensity, which is consistent with the known fact that the station located on the sedimentary rocks is more noisy than the station located on hard rock sites (Taylor et al. 2009).

MSM for a mud volcano near Mt. Karabetov suggested a correlation between the regional geodynamics and the fluid activity and traced the fluid migration pathways down to the depths of 15–25 km (Sobisevich et al. 2008). Also, fluid sources were clearly seen in the depth range of 3500–5000 m (Gorbatikov et al. 2008a, b). In another work (Gorbatikov et al. 2011), it has been shown that the Vladikavkaz Fault was probably a major seismogenerating structure as the deformations of young sediments were isolated by the MSM. The method was successfully tested on various breccia pipes (Gorbatikov et al. 2009; Danilov 2011; Popov et al. 2014). The results obtained for different breccia pipes were in good agreement with each other. The most obvious contradiction is the fact that the ore-controlling fault and pipe Marusinovskaya figured with the same intensity (Gorbatikov et al. 2009). In other cases, faults stand out as zones with higher contrast than pipes (Danilov 2011; Popov et al. 2014). On the other hand, the test tube explosion was located at different geological conditions, which may allow for such differences.

Due to the fact that the microseismic sounding method is aimed at the vertical and near-vertical boundaries, it can be used for the allocation of various geological objects, including faults and diatremes.

3. Particle Motion

The microseisms are background tremors caused by various sources. The microseismic motion consists of various types of seismic waves, however, the surface waves are dominating (Bath 1974). In the current work, analysis of particle motion in the Solid Earth was carried out in order to evaluate the validity of mathematical modeling results (Gorbatikov and Tsukanov 2011) as applied to real microseism. Data of permanent station PSS (located in the Arkhangelsk Region, Russia), VSU (GEOFON), RES (Canadian National Seismograph Network) (GEOFON), COLA (College Outpost, Alaska, USA) (USGS) were analyzed. Sources of low-frequency microseisms could be observed in a broad band.

According to Gorbatikov and Tsukanov (2011), the resolution ability and minimal size of imaged heterogeneity are proportional to the wavelength. These functions were observed as a result of amplification of Rayleigh wave. As consequence these functions have to reflect the particle motion.

Figure 2 shows that the peak of storm microseisms was observable in the frequency range of 0.18–0.32 Hz. In this frequency bandwidth, the particle motion had a random nature, indicating that the effect of different packets of waves was significant even if the signal exceeded the ambient level by two orders of magnitude.

Mathematical modeling showed that the wave changes the intensity when crossing heterogeneity more than 4% of the wavelength (Gorbatikov and Tsukanov 2011). For oscillation in the frequency range of 7–10 Hz, 4% of the wavelength corresponds to the frequency range of 0.2–0.4 Hz. For oscillation in the frequency range of 0.5–1 Hz, 4% of the wavelength corresponds to the frequency range of 0.02–0.04 Hz.

Mathematical modeling showed that the value of resolution is about 30% of the wavelength. For oscillation in the frequency range of 7–10 Hz, 30% of the wavelength corresponds to the frequency range of 2–3 Hz. For oscillation in the frequency range of 0.5–1 Hz, 30% of the wavelength corresponds to the frequency range of 0.2–0.3 Hz.

Figure 3 shows that the analysis of a narrower bandwidth (4% of the average frequency) allowed to identify a strict ellipsoidal particle motion with a smooth rotation of the polarization axis in time. The frequency band in the range of 30% of the average frequency provides rather a uniform rotation of the polarization axis and mainly ellipsoidal particle motion. In this case:

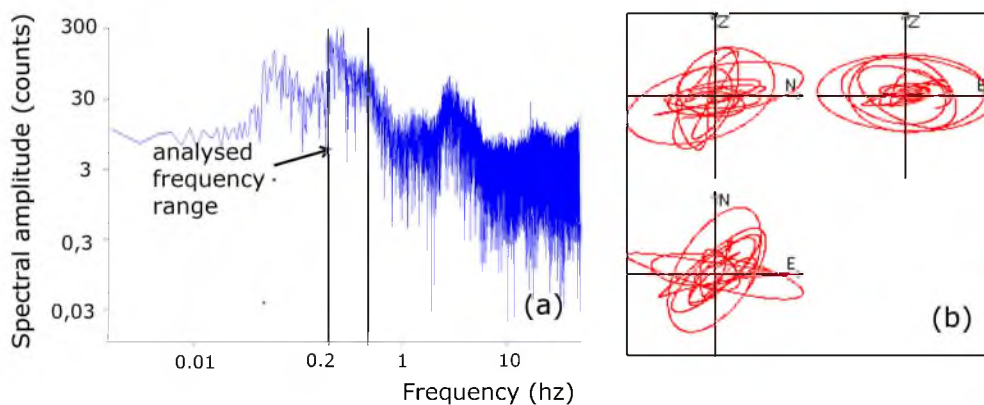


Figure 2
Microseism spectrum (a) and particle motion in frequency bandwidth 0.18–0.32 Hz (b)

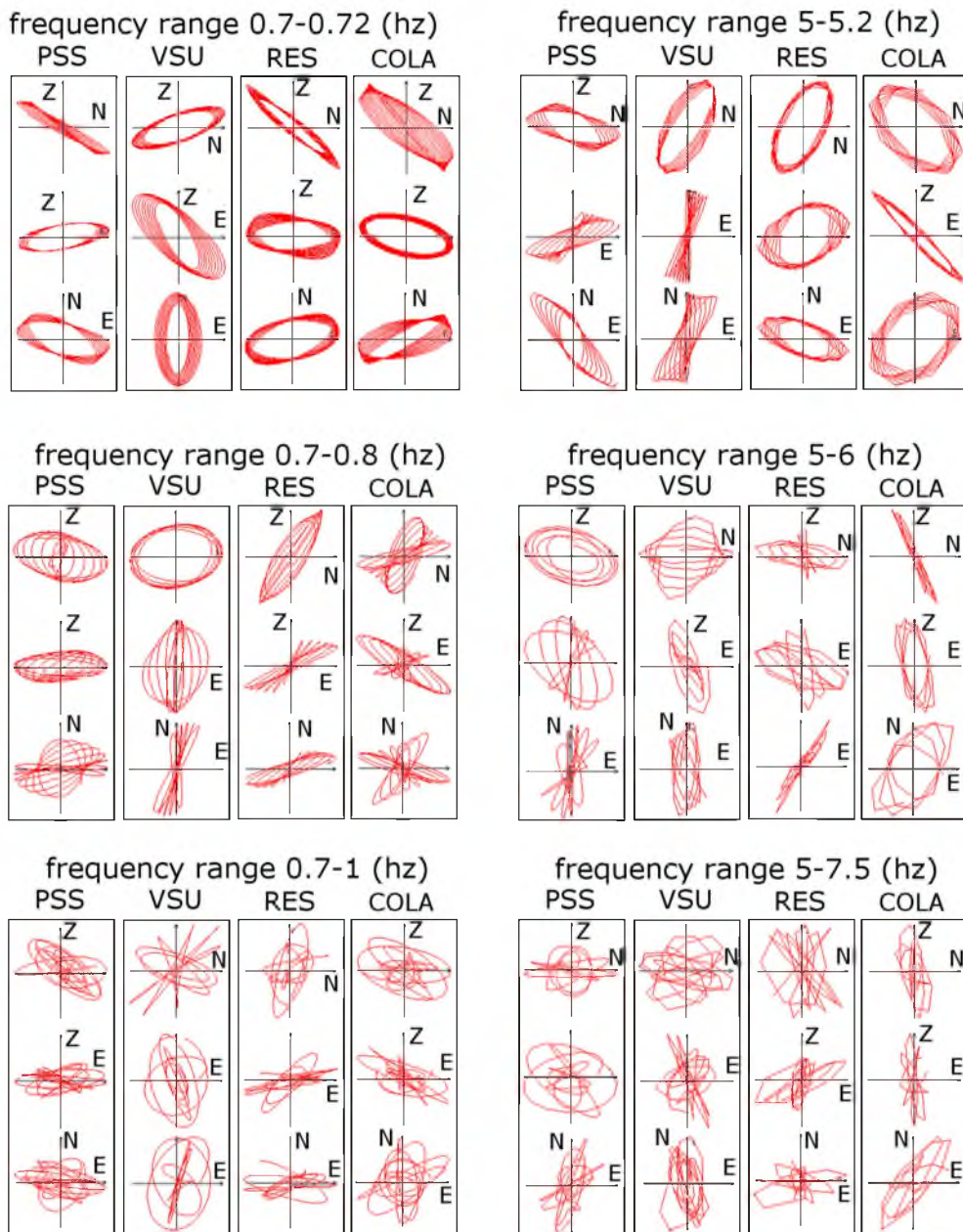


Figure 3
Microseism particle motion for different bandwidth frequencies according to the stations PSS, VSU, RES, COLA data

1. radius of the ellipse and the position of the polarization axis can be changed abruptly;
2. the motion of particles in the trajectory of motion is not only ellipsoidal.

These facts were observed both at low and at high frequencies according to different stations. As

consequence, the character of the particle motion is determined primarily by the proportion of analyzed wavelength.

The strict ellipsoidal particle motion with a smooth rotation of the polarization axis in time can be described by Lissajou curves emanating from the

superposition of two harmonic signals propagating perpendicular to each other. A gradual change in the position of the polarization axis of the Lissajou curves is observed when the signals differ from each other slightly (Jaworski and Detlaf 1981).

In a real situation, there are several sources, randomly distributed in space and with the phase difference, affecting the system simultaneously. Single trains can be clearly observed on the waveforms filtered in the narrow band of frequencies. Various amplitude, duration, and polarization indicate that each train has its own set of sources. On the other hand, the gradual change of the polarization axis shows that single train cooperates with the other.

Observed mechanism of particle motion can be explained as follows. The minimal wavelength range which is determined by the character of motion of the particles is 4% of the wavelength. Provisionally this range was named as an area of “cooperative” motion of the particles. If the observed wavelength range is less than 30% of the average wavelength, the wave trains of the areas of “cooperative” motion of the particles interact with one another. If the observed wavelength range is more than 30% of the average wavelength, the interaction between the areas of “cooperative” motion of the particles is nearly absent.

Reflection of the results of mathematical modeling on the character of particle motion indicates the reliability of the results.

4. Stability Assessment of Microseism

It is necessary to correct the application of the microseismic sounding method (MSM) that the intensity of microseisms was stable during the accumulation of a signal (Gorbatikov et al. 2008a, b).

Knowledge of the spectral amplitude accuracy allows to reasonably use the various methods of microseism analysis. In particular MSM accuracy depends on its parameters.

In the current work, the data of three regular seismic stations of the Arkhangelsk seismic network were analyzed: Franz Joseph Land (ZFI), Tamitsa (TMC), Klimovskaya (KLM). As shown in Fig. 1, the stations are distributed throughout the Arkhangelsk

region. ZFI seismic station is located on the Alexandra Land island of Franz Josef Land archipelago, and is the northernmost regular seismic station in Russia. TMC seismic station is located on the coast of the White Sea. KLM is situated in the continental part of Arkhangelsk region.

Examples of temporal variations of the spectral amplitudes of ZFI station is shown in Fig. 4. Figure 4 shows that the microseismic oscillation occurs mostly in a particular band of the spectral amplitudes. The average level of spectral amplitudes is smoothly variable of 40% for 10 h. The fact says that the variation in the microseism intensity happens with a certain regularity. As a consequence it is necessary to assess the relative error of the spectral amplitude measurement depending on the microseism accumulation period.

2011–2012 recording data were analyzed. It was selected in 30 intervals of records for microseism analysis. The interval recording duration was 4 h, which is the maximum period of stationarity (Gorbatikov and Stepanova 2008), above which determination of the spectral amplitude accuracy is meaningless. The vertical channel records were invoked in the analysis. Normal operation of the equipment and the lack of visible noise impacts on the waveforms in the majority of the duration of a record were chosen as an interval selection criteria. In the chosen intervals, fluctuations in the ranges of frequencies of 0.5–0.6, 0.6–0.7, 0.7–0.8, 0.8–0.9, 0.9–1, 1–1.2, 1.2–1.4, 1.4–1.6, 2.2–2.4, 8.4–8.6 Hz were filtered. Average values of spectral amplitudes

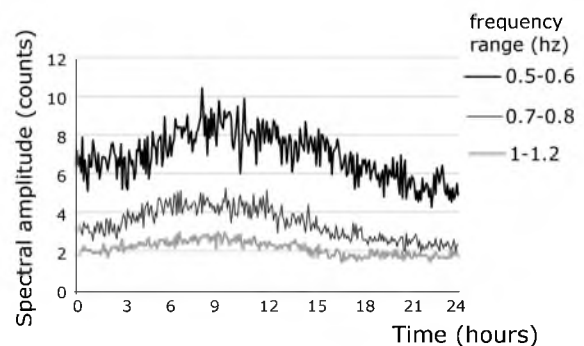


Figure 4

Variations of microseism spectral amplitudes according to the data by the station Franz Josef Land (ZFI) in different frequency ranges. a 0.5–0.6 Hz, b 0.7–0.8 Hz, c 1–1.2 Hz

were calculated for each 5 min in each frequency bandwidth. Calculations were made using the software package DAK (Popov et al. 2014). For the sake of simplicity of the material presented, we will continue to speak about the same frequency band, meaning that similar actions are performed for all bands. From henceforth the periods of accumulation of 30, 60, 90, and 240 min were considered. A mean error and a mean square error of the spectral amplitude were calculated for each accumulation period. Thus, the values of the relative error of the spectral amplitudes for 30, 60, 90, and 240 min accumulation for each interval were obtained. Gaps in each interval were excluded from the received values. For each station, the remaining set of values were averaged for each period of accumulation. Thus, the most probable values of a relative error of the spectral amplitudes for the periods of accumulation of a signal of 30, 60, 90, and 240 min were received. Results are presented in Fig. 5.

The result of the microseismic sounding method (MSM) is a distribution diagram of the relative intensity of microseisms. The relative intensity is calculated by the formula (1).

$$\Delta I = 17.37\delta A \quad (2)$$

The absolute error of the relative microseism intensity (ΔI) is directly proportional to the relative error of the spectral amplitude (δA). The calculated errors of the relative intensity are presented in Fig. 5.

Figure 5 shows that the increase in the signal accumulation period up to 4 h reduces the measurement error up to 3%. The largest errors occur when there is the signal accumulation for 30 min at frequencies higher than 2 Hz. It should be noted that the microseisms at frequencies up to 1.6 Hz differ from microseisms at higher frequencies.

Values of a relative error at frequencies of 0.5–1.6 Hz are close for all points and are equal to 3–8%. This fact is observed regardless of the distance from the sea areas and the availability of sources of industrial noise.

Error level at frequencies over 1.6 Hz is twice as many as the one at low frequencies, thus certain features for each point are observed. Diagrams for KLM and ZFI points which were obtained for frequencies 1.4–2.4 Hz (Fig. 5a, c) are very similar in

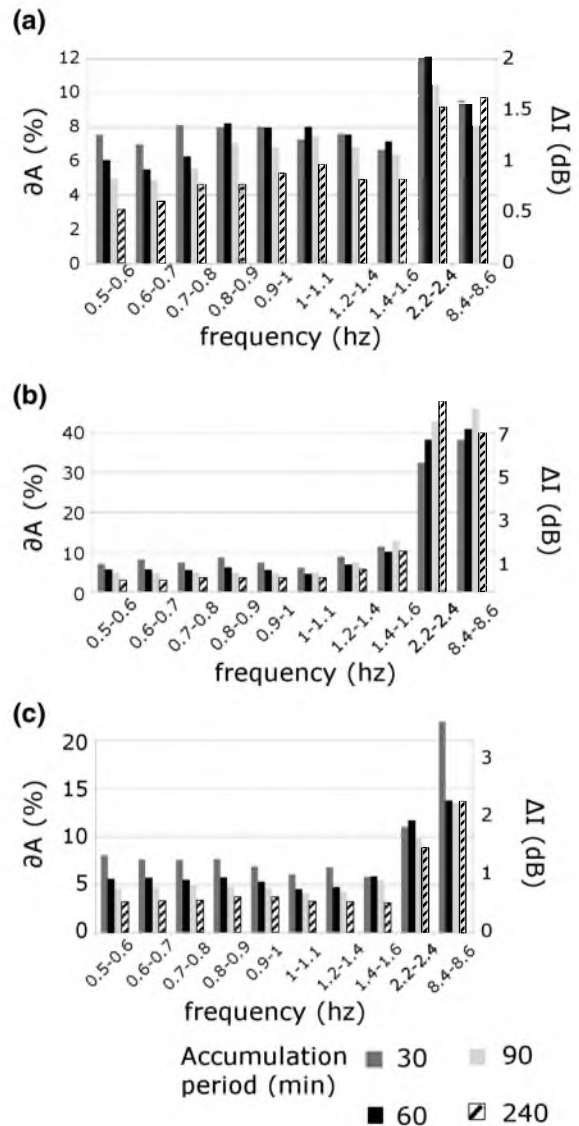


Figure 5

Diagrams of relative errors in the determination by spectral amplitude of microseism (δA) and by relative microseism intensity (ΔI , dB) in different frequency bands with different signal accumulation in time. Diagram constructs for permanent station of the Arkhangelsk seismic station network: **a** Klimovskaya (KLM); **b** Tamica (TMC); **c** Franz Josef Land (ZFI)

nature and values. The level of errors increases with increasing accumulation period of the signal from 30 to 60 min. The error decreases significantly with further increasing of the accumulation period up to 4 h. At lower frequencies, similar character of charts is observed only for “continental” KLM station at frequencies over 0.8 Hz. This character of the diagrams indicates the presence in the continent of

sufficiently stable oscillation of microseisms intensity with a period of about an hour. The error values of the ZFI point are slightly smaller than for the KLM points.

Obtained for mid frequencies in TMC point diagrams differ significantly from the other ones. This fact is caused by the prevalence of technogenic sources of microseisms over natural one, even at rather uniform waveforms. In favor of the last findings speaks the following two issues. Firstly, the error value in the TMC points is much higher than the ones in the other observation points. Secondly, the errors increase with the increasing accumulation period. This distribution can be observed only due to unpredictable changing of the set of intense sources. This fact indicates once again that microseisms at frequencies up to 1.6 Hz and above vary in their “stability” regardless of their source. The following man-made sources of microseisms in the TMC point can be considered: industrial site with a sawmill, a federal highway, and human activities in the nearest villages.

The diagrams of the ZFI and KLM points have differences in patterns. Also there are no anthropogenic influences in the points. The ratio of the error in KLM point to the corresponding values in ZFI point was calculated to compare the results. Figure 6 shows that the value of errors in the KLM point exceeds the corresponding values in the ZFI point. These differences are amplified by increasing the accumulation period. The biggest difference is observed at frequencies 1–1.2 Hz. The difference at the frequency of 0.5 and 2.3 Hz is practically not

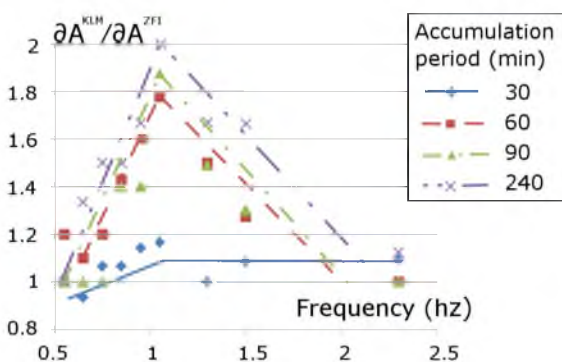


Figure 6

The ratio between values of relative errors in KLM points and corresponding values in ZFI points with different signal accumulations in time

observed. From the above it can be concluded that the frequency range of 0.8–1.6 Hz affected as “marine” and “continental” microseisms. The dominance of one or another source depends on the distance from the sea areas.

In spite of the fact that the accuracy of spectral amplitude determination can be close to 3%, in most cases, the most optimum period of accumulation is 1.5 h. So the accumulation of the signal within 1.5 h allows almost to achieve the precision limit with substantially smaller time consumption. The errors are 5 and 9% for microseism at frequency bands 0.5–1.6 Hz and 1.6–8.4 Hz, respectively.

In view of the direct relationship between each other, the accuracy of the relative intensity microseisms is characterized by the same rules that have been described for the relative error. Figure 5 shows that the relative intensity error is close to 1 dB for the accumulation of signal time of 1.5 h for the frequencies below 1.6 Hz. At the KLM and ZFI stations at frequencies above 1.6 Hz the errors are smaller than 2 dB. The increase of the accumulation period up to 4 h will reduce the error to 0.5–0.7 dB. Most parts of the errors (8 dB) are observed in the TMC point at frequencies higher than 2 Hz.

5. Field Work Procedure and Equipment

The Palovo–Samoded profile passes along the southern edge of the Arkhangelsk offset and the north-eastern edge of the Onega downthrown block (Fedorov 2004; Leonov 2010) (the Kandalaksho–Severodvinsky downthrown block; refer to Fig. 7). This profile includes a 20-point measurement of microseisms. Spacing between the points is 1.5–3 km. The GSR-24 seismic station with the CMG3-ESP velocimeter was used as a basis, and the UGRA-54 seismic station with the CM3-OS velocimeter was used as a mobile unit.

The Samoded–Malinovka profile crosses a known fault between the Onega downthrown block and Karelian offset at Point 37 (Leonov 2010), as shown in Fig. 7a. In this case, the depth of crystalline basement varies from 5 km at the beginning of the profile to 500 m at the end (Fig. 7a). According to another source (Fedorov 2004), it crosses a fault

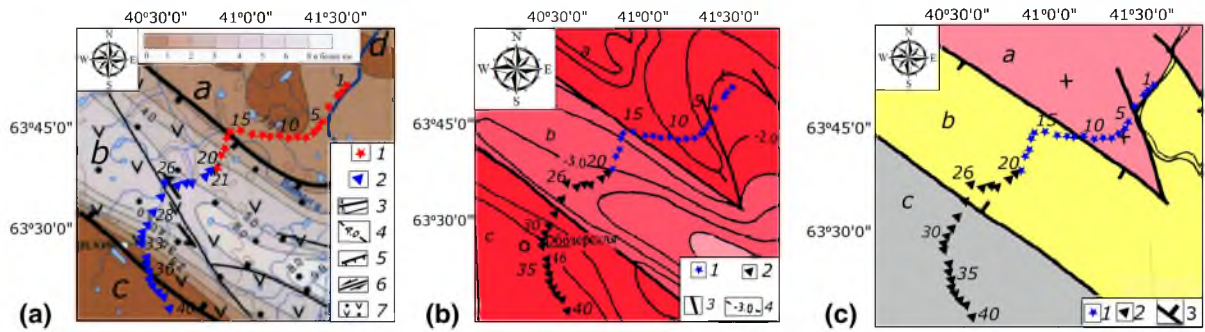


Figure 7

Geological map of the area of research showing the measurement points for the microseisms. **A** Tectonic map of the White Sea and adjacent territories (Leonov 2010); **B** a structural map of the surface of crystalline basement of the Mezen syncline (Fedorov 2004); **C** circuit potential of the Riphean tectonic zonation of the oil and gas complex of the Mezen sinekliza (Fedorov 2004): *a* Arkhangelsk offset; *b* the Onega downthrown block or the Kandalaksho–Severodvinsky downthrown block; *c* the Karelian offset or the Onega offset; *1* point of measuring the profile microseisms for Palovo–Samoded; 2 points of measuring the profile microseisms for Samoded–Malinovka; 3 faults: *a* bounding a large structure of the crust, *b* other; 4 isohypse surface of crystalline basement; 5 dumping break; 6 shift break; 7 volcanogenic–sedimentary complex downthrown block depression

between the Kandalaksho–Severodvinsky downthrown block and Onega offset at Points 27–28, as shown in Fig. 7b, c. In this case, the depth of crystalline basement varies from 3 km at the beginning of the profile to 500 m. The Samoded–Malinovka profile include a 20-point measurement of microseisms in steps of 1.5–3 km. As the reference we used a seismic station UGRA-54 with a velocimeter SM3-OS, and a mobile seismic station GSR-24 with a velocimeter CMG-40.

The depth was estimated to be 14.5 km. Thus, the processing involved the detection of frequencies above 0.1 Hz, which can be reliably detected.

Processing of records of microseisms was made by a specially developed software package, DAK (Popov et al. 2014).

6. Results and Discussion

The results of microseismic sounding method (MSM) processing are shown in Fig. 8. The Riphean deposits (Fedorov 2004) (points. 1–3, 12–27) were observed as zones with higher intensity. In the vicinity of Vendian deposits (Fedorov 2004) (points. 1–3, 6–9) (Fig. 8b), low-velocity zones were observed at depths from 1 down to 3 km.

Crystalline basement of Onega downthrown block appears as a high-intensity zone (Fig. 8). This fact

indicates low-velocity properties of the downthrown block and its fractured structure. The obtained data are consistent with the known geophysical information for the investigated area according to CMP data seismic velocity in the downtown block a third less than in Arkhangelsk offset (Kadyrova 2007). The northern boundary of the downthrown block in crystalline basement is shown by point 12, while, according to the data in Fig. 7, this boundary is crossed out at point 15.

Within the downthrown block there is a significant discrepancy between the data on the depth of the surface of crystalline basement obtained from different sources. Thus, the boundary reported in a previous work (Fedorov 2004) and also shown in Fig. 7b, passes through a high-speed layer (see Fig. 8) converging at a depth ranging from 1 to 4.3 km. In turn, according to Tectonic Map (Leonov 2010) (Fig. 7a), this boundary runs along the surface of contrasting high-intensity zone (Fig. 8), associated with the deep part of the Onega downthrown block and down to a depth of 1 km to a depth of 5 km.

According to the results of MSM, the southern boundary of the downthrown block most fully conforms to the data of Tectonic map (Leonov 2010). The southern boundary according to (Fedorov 2004) (Fig. 7b, c) is consistent with the high-intensity part of the Onega downthrown block at depths up to 2.5 km.

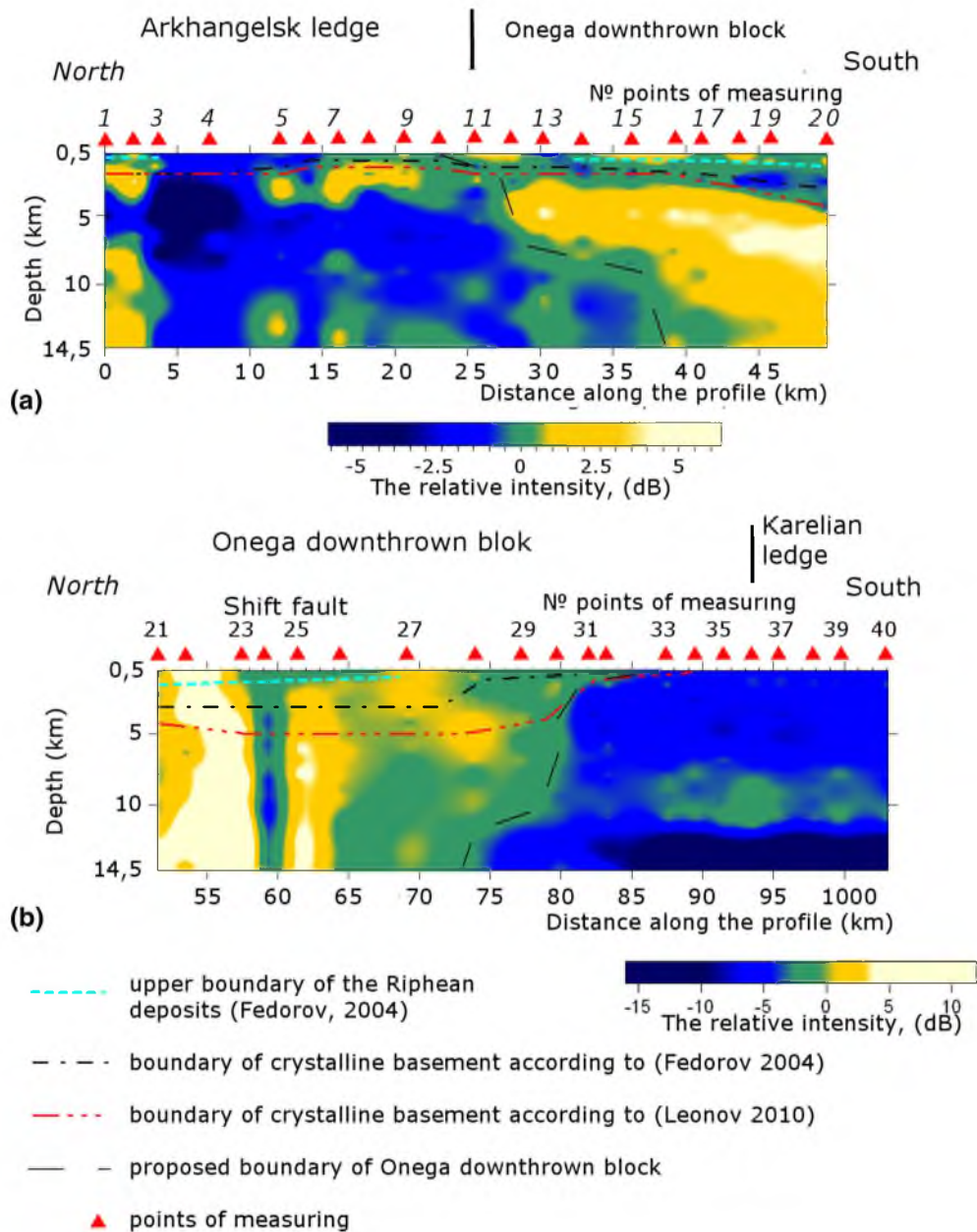


Figure 8

Geophysical cross sections along **a** Palovo–Samoded profile and **b** Samoded–Malinovka profile

The “super resolution” was observed for the intensity zones located between points 23 and 25. There, volcanogenic–sedimentary is abundant in the area of downthrown block (Fig. 7a). As a consequence, this image may be interpreted as ancient volcanoes at points 23 and 25. High-intensity zone indicated by points 22–23 is located not only in the

crystalline but in the sedimentary sheath, and it can serve as a beam transport of subsurface water, radon, and other elements. These conclusions are consistent with the previously reported data. The survey area is a passive continental margin. Its characteristic feature is the high tectonism, reflected in the lower part of the Upper Riphean. Within the Onega trough, volcanism

is also seen in the beginning of the Late Vendian (Maslov et al. 2002).

Two contrasting low-speed vertical zones at points 21–23 and 25 are most likely due to the shift fault (Leonov 2010). This zone is situated further to the south compared to the fault indicated at the Tectonic map (Leonov 2010) by points 26–27. Less contrast zone is shown at points 27–28, at depths down to 7 km. It should be noted that for zones at points 21–23 and 27–28, a shift to the North in the layer between the surfaces of crystalline basement allocated according to various data (Fedorov 2004; Leonov 2010) is observed. Horizontal displacement to the North of the northern boundary of the low-velocity block is observed within similar depths. It is possible to draw the following conclusions:

- the Onega downthrown block is partitioned into more corrugated the northern and more consolidated the southern parts by shift fault;
- massive material of the Onega downthrown block displaced horizontally to the North at depths ranging from 3 down to 5 km.

According to the Samoded–Malinovka profile it is possible to allocate a layer at a depth of 7–10 km. At these depths in the Karelian ledge the low-speed layer is shown. In turn, a horizontal shift of the southern board by 5 km to the North is observed at the low-velocity block at a depth of 10 km. Layer of the crust located deeper than 10 km is observed with higher contrast.

The changes in the configuration and in the intensity of the allocated zones allow to allocate the layers in the crust at depths of 0.5–3 km, 3–5 km, 5–7 km, 7–10 km. These conclusions are in line with the previously reported data (Egorkin 1987; Kostyuchenko et al. 2004; Vaganova 2012), demonstrating that the seismic horizons in the crust could be allocated at depths of 5, 7, and 10 km.

7. Conclusions

In the present work, the microseismic sounding method (MSM) was, for the first time, applied to obtain geological–geophysical information on the Arkhangelsk region located in the North–West

Russia. Investigation of particle motion character improves the validity of independent researches of MSM ability.

A stability study of microseisms allowed to determine that the error of the microseismic sounding method is 1–2 dB. Microseisms can be surely divided by the level of the spectral amplitude error at the frequency bands 0.5–1.6 Hz (5%) and higher (10%). Man-made microseisms were characterized by an error of 30–50%. Microseisms at frequencies of 8.4–8.6 Hz are characterized by a weak dependence on the period of accumulation and further study of the microseisms is required. The error in the determination of the relative microseism intensity is directly proportional to the relative error in the determination of the spectral amplitude with the coefficient of 17.37. As a result, the error in the determination of the relative microseism intensity for the frequencies 0.5–1.6 Hz is 1 dB and the one for frequencies 2–8.4 is approximately 2.5 dB. Even a weak man-made activity causes an error of 5–8 dB.

The results of our study confirmed the accuracy of independent research on the most optimal signal accumulation period of 1.5 h. The increase of the accumulation period duration from 1.5 to 4 h will cause reduction of the spectral amplitude error by 2% and reduction of the relative microseism intensity errors by 0.2 dB.

If we assume that the majority of structural elements of the crust and faults were imaged with the relative intensity of more than 1 dB (Gorbatikov et al. 2008a, b, 2013; Sobisevich et al. 2008; Danilov 2011; Popov et al. 2014), then it is possible to claim about possibility of using the microseismic sounding method.

The method allowed us to clarify the position of the sub-vertical boundaries of geological objects such as boundaries of structural elements, faults, and their components blocks. The present findings were consistent with the known geological and geophysical information. Of particular importance were the findings demonstrating that all boundaries indeed exist in the environment despite the disagreement in the literature on the situation of the crystalline basement and the downthrown block boundary. Due to the complex structure of the investigated system, it was, however, difficult to clearly define which of the

allocated boundaries were the structural element boundaries and which were the boundaries of the component blocks. The main reasons causing the dissonance of geology information are:

- that the downthrown block is divided into the northern and southern blocks;
- there is a horizontal displacement in the layer to the North at depths ranging from 3 down to 5 km.

It was shown that the most reliable data were presented in the Tectonic map (Leonov 2010). However, additional investigation would be needed to draw a more accurate conclusion. The obtained information allows for a more complete description of the structure and physical properties of the environment. As a consequence, we can assert the applicability of the microseismic sounding method to refine the existing geophysical information. The results confirm the high horizontal resolution and sensitivity to the fractured rocks. These features are very important for the study of different critical zones (Parsekian et al. 2015).

Acknowledgements

Dr Danil Korelskiy and Danilov Mikhailare are gratefully acknowledged for the language help. The discussions with Dr A. V. Gorbatiykov, Dr V. I. Francuzova, Dr A. N. Morozov, Yu. N. Afonin, and A. V. Koshkin were very helpful. This work was carried out as a part of the research project of Federal Agency for Scientific Organizations, project no AAAA-A16-116052710111-2.

REFERENCES

Asten, M. W. (1978). Geological control on the three-component spectra of Rayleigh-wave microseisms. *Bulletin of the Seismological Society of America*, 68, 1623–1636.

Asten, M. W., & Henstridge, J. D. (1984). Array estimators and the use of microseisms for of sedimentary basins. *Geophysics*, 49, 1828–1837.

Bath, M. (1974). *Spectral analysis in geophysics*. Amsterdam: Elsevier.

Bonnefoy-Claudet, S., Cotton, F., & Pierre-Yves, Bard. (2006). The nature of noise wavefield and its applications for site effects studies: A literature review. *Earth-Science Reviews*, 79, 205–227. doi:10.1016/j.earscirev.2006.07.004.

Dalton, C. A., & Ekström, G. (2006). Constraints on global maps of phase velocity from surface-wave amplitudes. *Geophysical Journal International*, 167, 820–826. doi:10.1111/j.1365-246X.2006.03142.x.

Dalton, C. A., Hjørleifsdóttir, V., & Ekstrom, G. (2014). A comparison of approaches to the prediction of surface wave amplitude. *Geophysical Journal International*, 196(1), 386–404. doi:10.1093/gji/ggt365.

Danilov, K.B. (2011). Application of microseismic sounding for the study of Lomonosov diatremes (Arkhangelsk diamondiferous province), *Bulletin of the Kamchatka regional organizations educational and scientific center. Series: Earth Science*, 17, 231–237. http://www.kscnet.ru/kraesc/2011/2011_17/2011_17.html.

Eddy, C. L., & Ekström, G. (2014). Local amplification of Rayleigh waves in the continental United States observed on the USArray. *Earth and Planetary Science Letters*, 402, 50–57.

Egorkin, A.V. (1987). Structure of the crust and upper mantle along profiles Cheshskaya Bay—Pay-Khoy Ridge, the White Sea—Vorkuta, the Dvina Bay—the Mezen River, the river Onega—Cheshskaya Bay, river Vaga—the White Sea. *The report of cameral party of Special Regional Geophysical Expedition on results of the regional seismic researches DSS, reflection method which are carried out in 1985–1987 in the north of the European part of the USSR (in two books)*. Sheets R-39, 40,41, 42; Q-37, 38, 39, 40, 41; P-37, 38. Moscow, DC: Special Regional Geophysical Expedition.

Fedorov, D.L. (2004). *Results of regional geological and geophysical work in Mezenskaya syncline in 2000–2001*. Moscow, DC: performance report by ZAO “Valdaygeologiya” Federal State Institution State Research and Production Enterprise “Spetsgeofizika”.

Francuzova, V.I., Makarov, V.I., & Danilov, K.B. (2013). Velocity heterogeneity of crust of southeast Belomorya according to a method of microseismic sounding, *Geophysical investigations*, 14, 47–55. <http://gr.ifz.ru/soderzhanie/tom-14-nomer-3-2013/>.

GEOFON [Electronic resource] <http://geofon.gfz-potsdam.de/geofon/>. Accessed 20 May 2014.

Gorbatiykov, A. V., Larin, N. V., Moiseev, E. I., & Belyashov, A. V. (2009). The microseismic sounding method: Application for the study of the buried diatreme structure. *Doklady Earth Sciences*, 428(1), 1222–1226. doi:10.1134/S1028334X0907040X.

Gorbatiykov, A. V., Montesinos, F. G., Arnos, J., Stepanova, M Yu., Benavent, M., & Tsukanov, A. A. (2013). New features in the subsurface structure model of El Hierro Island (Canaries) from low-frequency microseismic sounding: an insight into the 2011 Seismo-Volcanic Crisis. *Surveys In Geophysics*, 34, 463–489. doi:10.1007/s10712-013-9240-4.

Gorbatiykov, A. V., Ovsyuchenko, A. N., Rogozhin, E. A., Stepanova, M Yu., & Larin, N. V. (2011). The structure of the Vladikavkaz Fault Zone based on the study utilizing a complex of geological-geophysical methods. *Seismic Instruments*, 47(4), 307–313. doi:10.3103/S0747923911040037.

Gorbatiykov, A. V., & Stepanova, M. J. (2008). Statistical characteristics and stationarity properties of low-frequency seismic signals. *Izvestiya, Physics of the Solid Earth*, 44(1), 50–59. doi:10.1007/s11486-008-1007-0.

Gorbatiykov, A. V., Sobisevich, A. L., & Ovsyuchenko, A. N. (2008a). Development of the model of the deep structure of Akhtyr flexure-fracture zone and Shugo mud volcano. *Doklady*

- Earth Sciences*, 421(2), 969–973. doi:10.1134/S1028334X0806024X.
- Gorbatikov, A. V., Stepanova, M. J., & Korablev, G. E. (2008b). Microseismic field affected by local geological heterogeneities and microseismic sounding of the medium. *Izvestiya, Physics of the Solid Earth*, 7, 577–592. doi:10.1134/S1069351308070082.
- Gorbatikov, A. V., & Tsukanov, A. A. (2011). Simulation of the Rayleigh waves in the proximity of the scattering velocity inhomogeneities. Exploring the capabilities of the microseismic sounding method. *Izvestiya, Physics of the Solid Earth*, 4, 354–369. doi:10.1134/S1069351311030013.
- Horike, M. (1985). Inversion of phase velocity of long-period microtremors to the S-wave-velocity structure down to the basement in urbanized areas. *Journal of Physics of the Earth*, 33, 59–96.
- Jaworski, B. M., & Detlaf, A. A. (1981). *Handbook of physics*. Moscow: Nauka.
- Kadyrova, E.R., Smirnov O.A., Tkachenko K. Yu., & et al. (2007). Report “Support fieldwork, processing and integrated interpretation of seismic exploration CMP-2D Arkhangelsk licensed site”. Arkhangelsk region, Q-37, P-37. Moscow, DC: JSC “Pangaea”.
- Kanai, K., & Tanaka, T. (1954). Measurement of the microtremor. *Bulletin of the Earthquake Research Institute. The University of Tokyo*, 32, 199–209.
- Katz, L. J., & Bellon, R. S. (1978). Microtremor site analysis study at Beatty, Nevada. *Bulletin of the Seismological Society of America*, 68, 757–765.
- Kostyuchenko, S.L., Zolotov, E.E., & Rakitov, V.A. (2004). Sites of profiles Quartz and Ruby, in ed. Sharov, N.V. (Ed.): *Deep structure and seismicity of the Karelian region and its margins* (pp. 76–85) Petrozavodsk: Karelian Research Center, Russian Academy of Sciences.
- Leonov, M.G. (2010). Tectonic map of the White Sea and adjacent areas in the scale of 1:1500000. GS Kazanin, Moscow: LLC “IPP Kuna”.
- Lin, F.-C., Tsai, V. C., & Ritzwoller, M. H. (2012). The local amplification of surface waves: a new observable to constrain elastic velocities, density, and anelastic attenuation. *Journal of Geophysical Research*, 117, B06302. doi:10.1029/2012JB009208.
- Maslov, A. V., Olovyanishnikov, V. G., & Isherskaya, M. V. (2002). Rifev eastern, north-eastern and northern periphery of the Russian platform and the western Urals megazone: litostratigrafiya, formation conditions and types of sedimentary sequences. *Litosfera*, 2, 54–59.
- Monakhov, F. I. (1977). *Low-frequency seismic noise of the earth*. Moscow: Nauka.
- Nogoshi, M., & Igarashi, T. (1971). On the Amplitude Characteristics of Microtremor (Part 2) (in Japanese with English abstract). *Journal of the Seismological Society of Japan*, 24, 26–40.
- Parsekian, A. D., Singha, K., Minsley, B. J., Holbrook, W. S., & Slater, L. (2015). Multiscale geophysical imaging of the critical zone. *Reviews of Geophysics*, 53, 1–26. doi:10.1002/2014RG000465.
- Popov, D. V., Danilov, K. D., Zhostkov, R. A., Dudarov, Z. I., & Ivanova, E. V. (2014). Processing the digital microseism recordings using the Data Analysis Kit (DAK) software package. *Seismic Instruments*, 50, 75–83. doi:10.3103/S074792391401006X.
- Rawlinson, N., Pozgay, S., & Fishwick, S. (2010). Seismic tomography: A window into deep Earth. *Physics of the Earth and Planetary Interiors*, 178, 101–135. doi:10.1016/j.pepi.2009.10.002.
- Sobisevich, A. L., Gorbatikov, A. V., & Ovsuchenko, A. N. (2008). Deep structure of the Mt. Karabetov Mud volcano. *Doklady Earth Sciences*, 422(1), 1181–1185. doi:10.1134/S1028334X08070428.
- Taylor, S. R., Gerstoft, P., & Fehler, M. C. (2009). Estimating site amplification factors from ambient noise. *Geophysical Research Letters*, 36, L09303. doi:10.1029/2009GL037838.
- USGS Albuquerque Seismological Laboratory [Electronic resource] <http://earthquake.usgs.gov/regional/asl/>. Accessed 20 May 2014.
- Vaganova, N. V. (2012). A structure of crust and the top cloak of the North of the Russian plate on supervision of exchange waves from teleseismic earthquakes. The abstract of the thesis on competition of an academic degree of the candidate of geological and mineralogical sciences. (Yekaterinburg).
- Vinnik, L. P. (1968). *The structure microseisms and some questions of grouping methodology*. Moscow: Nedra.

(Received August 12, 2016, revised March 13, 2017, accepted March 27, 2017, Published online April 9, 2017)